# Diffractionless Flow of Light in All-Optical Microchips

Alongkarn Chutinan, Sajeev John, and Ovidiu Toader
*Department of Physics, University of Toronto, 60 St. George Street, Toronto, Ontario, Canada M5S-1A7*
(Received 17 May 2002; published 24 March 2003)

We introduce the concept of a hybrid 2D–3D photonic band gap (PBG) heterostructure which enables both complete control of spontaneous emission of light from atoms and planar light-wave propagation in engineered wavelength-scale microcircuits. Using three-dimensional (3D) light localization, this heterostructure enables flow of light without diffraction through micron-scale air waveguide networks. Achieved by intercalating two-dimensional photonic crystal layers containing engineered defects into a 3D PBG material, this provides a general and versatile solution to the problem of "leaky modes" and diffractive losses in integrated optics.

DOI: 10.1103/PhysRevLett.90.123901 PACS numbers: 42.70.Qs, 78.20.Ci

Diffraction is a fundamental property of light propagation in confined geometries. While guiding of light can be achieved through total internal reflection in a high refractive index medium, scattering and diffraction losses are inevitable whenever the translational symmetry of the guiding structure is broken. In general, this precludes the possibility of truly lossless microcircuits for light which could perform functions analogous to microelectronic circuits. Photonic band gap (PBG) materials are a special class of periodically modulated dielectrics which enable the localization or trapping of light [1,2]. Using carefully engineered modifications of the lattice translational symmetry, PBG materials enable microscopic molding of the flow of light without recourse to the refractive index guiding mechanism. While the potential for high quality PBG materials as base media for integrated all-optical microcircuits has been alluded to [3–5], neither an explicit demonstration nor a theoretical blueprint of a 3D optical microchip has been presented up to now. Here we provide a general and versatile solution to this central problem. Our prescription involves the stacking of planar integrated microcircuits for light through engineered defects in 3D PBG heterostructures. These circuits include linear air waveguides, micron-scale air guide bends, and microcavities which, unlike their counterparts in 2D photonic crystal slabs [6–10], do not suffer uncontrolled attenuation from "leaky modes." In our heterostructure, diffractive losses are eliminated by the complete removal of "final states" into which light could in principle scatter. By stacking planar microchips separated by roughly five unit cells of the 3D PBG cladding, our architecture enables integration of a large number of optical devices, each occupying less than 100 unit cells of the plane, operating at a wavelength of 1.5 $\mu$m.

In addition to 3D control of diffractive effects, light localization enables molding of light flow on a micron-scale through paths composed of air rather than dielectric material. Air waveguides have advantages over dielectric waveguides since they can remain single mode for the entire band gap and exhibit high transmission through suitably engineered sharp bends [9,11–14]. Our architecture for large scale optical microcircuits is extremely versatile. The intercalating 2D photonic crystal (PC) microchips can consist of a square or triangular lattice containing a wide variety of defects and circuit elements. Likewise, the host 3D PBG material can be chosen [15] from many known structures such as woodpiles [4,16], square spirals [17–20], or face centered cubic lattices [21,22]. The main requirement is simply that of a lattice match between the 2D PC and the plane across which this attaches to the surrounding 3D PBG.

For concreteness, we first illustrate a heterostructure based on the inverse square spiral 3D PBG structure, recently proposed for large scale microfabrication on the optical wavelength scale [17,18]. The fabrication process begins with a silica ($SiO_2$) template [Fig. 1(a)] of the square spiral structure, created by glancing angle deposition (GLAD) [19,20] onto a square array of seed posts of lattice constant $a$. This glass crystal consists of interleaving, square spiral arms (with transverse arm length of $1.5a$, vertical period of $1.7a$, and circular cross section of $0.33a$) which wind in phase with each other, arrayed on a 2D square lattice. A planar defect layer is deposited (after an integer number of square spiral unit cells has been created) by growth of a capping layer (solid slab) [18]. After the slab is grown to a desired thickness (in our case $0.5a$), it is patterned [as shown in Fig. 1(a)] in two separate steps (from the top surface). In the first step, a new 2D array of seed posts (of lattice constant $a$) is etched on the top surface to enable further growth of square spirals using GLAD. In the second step, the template for 2D microcircuitry is created by patterning the spaces between the seed posts with an array of circular holes (of diameter $0.34a$, in our case) that pass through the entire slab. Using standard microlithography, the slab can be made into a 2D PC with prescribed defects. Using an appropriate mask, holes can be absent along prescribed channels, leading to air waveguide circuits in the inverted structure. Also, isolated holes, with different radii than those of the background 2D PC, can be created to serve as

  

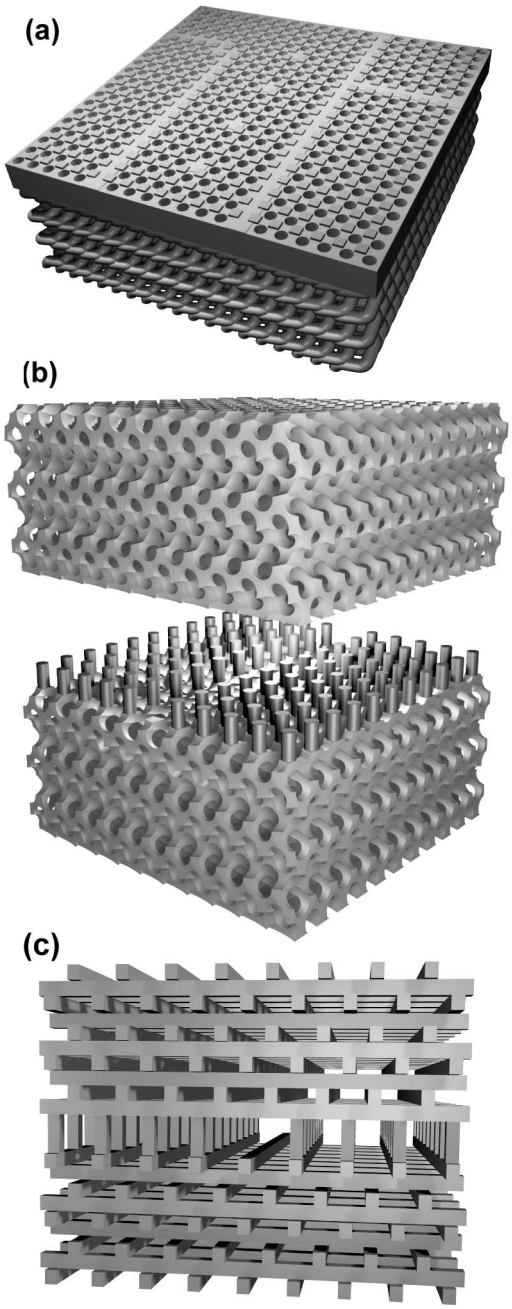


FIG. 1. (a) Template for the square spiral heterostructure consisting of a capping layer grown on top of a square spiral photonic crystal. The "inverse" structure consisting of air spirals in a Si background is depicted in (b). The upper 3D PBG cladding is separated to help visualize the 2D PC layer. A linear waveguide (missing row of rods) is depicted in the 2D microchip. (c) The analogous woodpile based heterostructure. The 2D PC consists of a square lattice of square rods. A single mode air waveguide is created by removing one row of square rods.

microresonators. The GLAD process is then repeated on the patterned slab with the new square spiral posts growing around the same axis of rotation and in the same sense as the posts below. Self-shadowing effects ensure that spiral posts grow from the seed posts without being affected by the preceding patterning of the 2D microchip. Finally, the entire glass template is infiltrated with silicon (or some other high refractive index semiconductor) using chemical vapor deposition and inverted [21,22] leaving behind an inverse square spiral PBG material sandwiching the planar defect layer with its optical microcircuit [see Fig. 1(b)]. We note that the 2D PC layer is inserted at the plane that cuts the square spiral precisely at the elbow. It has been shown previously [17] that this inverse square spiral, when made of silicon with dielectric constant 11.9, has a 3D PBG of 24%. Preliminary microfabrication results have also been presented elsewhere [18].

The photonic band structure of this heterostructure, calculated by the plane wave expansion method [23] in a supercell, reveals an on-chip, complete PBG over the frequency range $(0.339–0.369)a/\lambda$ for the 2D PC layer thickness of $0.5a$. In Fig. 2 we show only the in-plane modes created by the planar defect since the PBG excludes all other modes. These in-plane modes are contained within the 3D PBG of the cladding square spiral photonic crystal, leading to a decrease of the on-chip PBG of the heterostructure with increasing slab

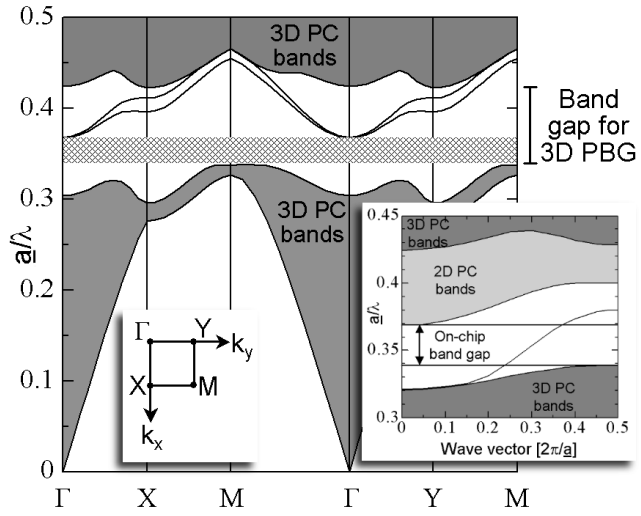


FIG. 2. Photonic band structure for the inverted optical heterostructure, in the absence of on-chip air waveguides or point defects. The dark shaded region corresponds to frequency bands of propagating electromagnetic modes while the frequency range $(0.339–0.423)/\lambda$ (shown in white) is the full PBG for the bulk 3D (silicon based) inverse square spiral PC. The hatched region $[(0.339–0.369)a/\lambda]$ shows the on-chip 3D PBG obtained after insertion of the 2D PC layer. In the frequency range $(0.369–0.423)a/\lambda$, all propagating modes are confined to the 2D PC layer. The inset shows the band structure and electromagnetic dispersion relation for an air waveguide channel within the 2D PC obtained by removing one row of dielectric rods [see Fig. 1(b)] in the 2D PC layer. The lightly shaded region indicates the frequencies of propagating modes in the 2D PC layer.

thickness. The on-chip PBG vanishes when the slab thickness reaches $0.8a$.

We introduce a linear air waveguide into the heterostructure by patterning the (template) slab to leave out a row of dielectric rods in the (inverted) 2D PC layer. The light is localized (in-plane) in air by the stop gap of the 2D PC layer and localized vertically by the 3D PBG of square spiral cladding layers. Shown in the inset of Fig. 2 is a band diagram for the waveguide mode when the thickness of the 2D PC slab is $0.5a$. It is seen that the air waveguide is single mode and spans the entire portion of the 3D PBG outside the bands of the 2D PC. By varying the thickness of the 2D PC slab, we find a tradeoff between the size of the on-chip PBG and the air waveguide dispersion. For a very thin slab, the on-chip PBG is large but the air waveguide mode is flat and spans only a short range of frequencies. For a very thick slab, the on-chip PBG is very small. By choosing a slab thickness of $0.5a$, the air waveguide mode precisely spans the on-chip PBG of 8.5% and exhibits a band center group velocity of $0.226c$. We use the 3D finite difference time domain (FDTD) method [24] (with ten points per lattice constant $a$) to calculate the field patterns of waveguide modes. Figure 3 shows the electric field of the wave with initial wave vector $k_x = 0.33\pi/a$ passing through the bend. The 3D light localization within our PBG facilitates the nearly perfect transmission of light around a sharp 90° bend in the air waveguide without leakage into the third dimension. With four unit cells of inverse square spiral above and below the microchip, the transmission and reflection spectra, obtained by Fourier transforming the pulses, reveals that more than 97% of the light is transmitted, less than 3% is reflected, and less than 0.5% remains unaccounted throughout the on-chip PBG, whose bandwidth (for a band centered at 1.55 $\mu$m) is 130 nm.

The 3D light localization in our microchip enables light passing through the air waveguide to interact with very high quality microresonators placed in proximity to the waveguide. For illustration, we consider a small refractive index defect displaced by $2a$ from the air waveguide as shown in Fig. 4. In addition, the coupling efficiency between the air waveguide and the microresonator is adjusted by reducing the dielectric constant of the intervening rod. While the quality ($Q$ factor) of an isolated microresonator in a 3D PBG is arbitrarily large, we choose $Q = 140$ in order to reduce the interaction time between the waveguide and resonator in our computations. The 3D FDTD calculations of the light propagating through this waveguide reveal that the transmission drops to 0% and the reflection becomes $\approx 100\%$ at the resonant frequency of $0.352/\lambda$. Unlike the corresponding result for a 2D PC slab, there is no leakage of light into the third dimension.

As mentioned above, the concept of the hybrid 2D–3D heterostructure can also be applied to different types of

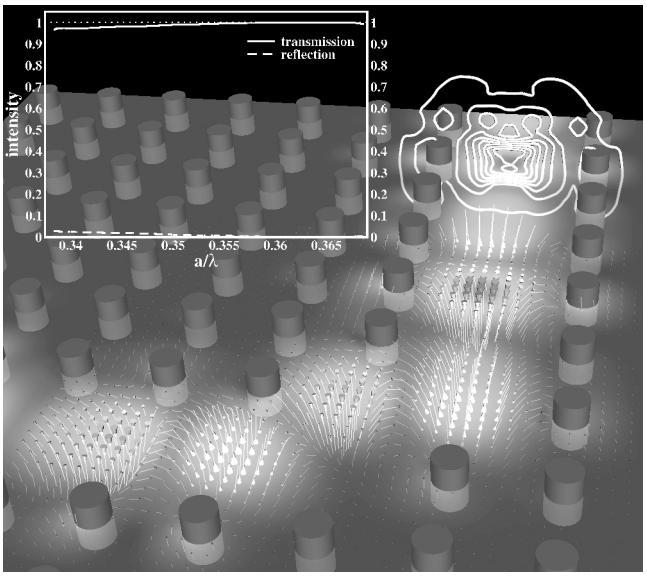


FIG. 3. An on-chip air waveguide inside the heterostructure of Fig. 1(b) allows transmission of electromagnetic signals around a sharp 90° bend. The 3D PBG material on top and bottom is not shown. The electric field is sampled on a horizontal plane which bisects the 2D PC layer. The plane is color coded according to the electric field intensity, where dark and bright correspond to low and high intensity, respectively. The arrows indicate the direction of the electric field vectors along various field lines. The mode exhibits a transverse magnetic character in regions where the intensity is highest. The equal intensity contours (white) in the vertical cross section of the waveguide are also illustrated. The transmission and reflection properties of the bend, shown in the inset, reveal nearly perfect transmission over a bandwidth of more than 130 nm for wavelengths near 1.5 $\mu$m.

PBG structures. Here we describe results for a heterostructure based on a pair of (3D) PBG woodpile structures [4,16] which sandwich a planar (2D) microchip consisting of square rods on a square lattice. For concreteness, we choose a woodpile cladding structure consisting of stacking rods with a rectangular cross section. The width and height of rods are $0.25a$ and $0.3a$, respectively, where $a$ is the distance between two adjacent rods in the same layer [see Fig. 1(c)]. As usual [25], one unit cell of the woodpile consists of four stacking layers. Thus, the vertical periodicity in the stacking direction is $1.2a$. For a dielectric constant of 11.9, this structure exhibits a complete 3D band gap from $a/\lambda \approx 0.365$–$0.438$. For the 2D PBG layer, square rods with width of $0.25a$ are chosen to structurally match with the woodpile structure. The square lattice of square rods is inserted between a pair of adjacent layers of the woodpile, and the original pair of woodpile layers is now separated by the height of the intercalating rods [see Fig. 1(c)]. One rod is placed at each of the square lattice points defined by crossing points of the adjacent woodpile layers. We choose the thickness of the 2D PBG layer as $0.8a$ and obtain an on-chip PBG

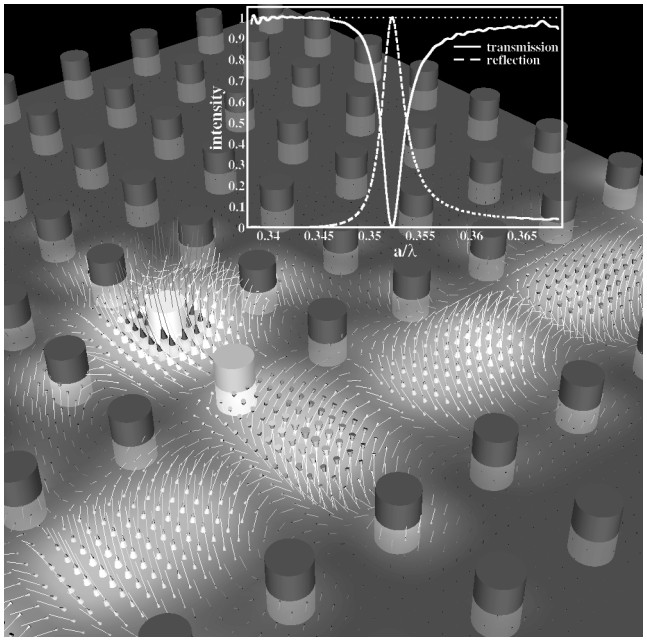


FIG. 4. Air waveguide mode resonantly coupled to a point defect (microcavity) on the optical microchip is depicted. The inverse square spiral PBG material above and below is not shown. The defect is created by changing the dielectric constant of one rod in the vicinity of the waveguide from 11.9 to 1.5 ($2a$ from the waveguide). The dielectric constant of the adjacent rod (also adjacent to the waveguide) is adjusted to 5.9 for computational convenience. The electric field intensity and electric field vectors (color coded as in Fig. 3) provide a steady state snapshot ($a/\lambda = 0.352$) of the field configuration from a point source placed at the center of the $\epsilon = 1.5$ rod. The inset shows results from a separate calculation of transmission and reflection spectra of light sent along the waveguide from a source placed a large distance away from the defect.

from $\underline{a}/\lambda \approx 0.365$–$0.391$. The air waveguide mode then spans the entire range of the on-chip PBG. We have also calculated the transmission and reflection spectra for the waveguide bend in this heterostructure. The 3D FDTD calculations reveal diffractionless transmission of more than 99% for almost the entire on-chip PBG and the reflection of less than 0.3% for the same range. Similar results [15] apply to the face centered cubic lattice 3D PBG structure obtained by drilling a triangular lattice of sets of three (criss-crossing) cylindrical pores throughout a bulk dielectric material [26]. In this case, our intercalating planar microchip consists of circular rods in a triangular (2D) lattice.

In summary, we have demonstrated a nearly universal approach to diffractionless integrated optics in a 3D PBG material, amenable to low cost microfabrication using established deposition and etching techniques. Using 3D light localization, our microchip facilitates air waveguide based circuits for light on the micron scale and provides additional control of spontaneous emission from light emitters placed within active regions of the chip. For example, it has been suggested that a low threshold all-optical microtransistor could be realized if a large collection of two level atoms (quantum dots) is placed at suitable locations within such a microchip where the local electromagnetic density of states exhibits a sharp steplike discontinuity [27]. The integration of these and other active devices into this optical microchip could lead to all-optical functionality rivaling and perhaps exceeding that of current day microelectronics.

This work was supported in part by the Natural Sciences and Engineering Research Council of Canada.

[1] S. John, Phys. Rev. Lett. **58**, 2486 (1987).
[2] E. Yablonovitch, Phys. Rev. Lett. **58**, 2059 (1987).
[3] J. D. Joannopoulos, P. R. Villeneuve, and S. Fan, Nature (London) **386**, 143 (1997).
[4] S. Noda *et al.*, Science **289**, 604 (2000).
[5] M. L. Povinelli *et al.*, Phys. Rev. B **64**, 075313 (2001).
[6] S.-Yu Lin *et al.*, Appl. Phys. Lett. **68**, 3233 (1996).
[7] T. Baba, N. Fukaya, and J. Yonekura, Electron. Lett. **35**, 654 (1999).
[8] S. G. Johnson *et al.*, Phys. Rev. B **60**, 5751 (1999).
[9] A. Chutinan and S. Noda, Phys. Rev. B **62**, 4488 (2000).
[10] S. Noda, A. Chutinan, and M. Imada, Nature (London) **407**, 608 (2000).
[11] A. Mekis *et al.*, Phys. Rev. Lett. **77**, 3787 (1996).
[12] M. M. Sigalas *et al.*, Microw. Opt. Technol. Lett. **23**, 56 (1999).
[13] A. Chutinan and S. Noda, Appl. Phys. Lett. **75**, 3739 (1999).
[14] M. Bayindir *et al.*, Phys. Rev. B **63**, 081107(R) (2001).
[15] A. Chutinan, S. John, and O. Toader (to be published).
[16] S. Y. Lin *et al.*, Nature (London) **394**, 251 (1998).
[17] O. Toader and S. John, Science **292**, 1133 (2001).
[18] S. R. Kennedy *et al.*, Nano Lett. **2**, 59 (2002).
[19] K. Robbie and M. J. Brett, J. Vac. Sci. Technol. B **15**, 1460 (1997).
[20] K. Robbie, J. C. Sit, and M. J. Brett, J. Vac. Sci. Technol. B **16**, 1115 (1998).
[21] A. Blanco *et al.*, Nature (London) **405**, 437 (2000).
[22] Hernan Miguez *et al.*, Adv. Mater. **13**, 1634 (2001).
[23] K. M. Ho, C. T. Chan, and C. M. Soukoulis, Phys. Rev. Lett. **65**, 3152 (1990).
[24] K. S. Yee, IEEE Trans. Antennas Propag. **14**, 302 (1966).
[25] K. M. Ho *et al.*, Solid State Commun. **89**, 413 (1994).
[26] E. Yablonovitch, T. J. Gmitter, and K. M. Leung, Phys. Rev. Lett. **67**, 2295 (1991).
[27] S. John and M. Florescu, J. Opt. A: Pure Appl. Opt. **3**, S103 (2001).